

Reprinted with permission from: Jamard M, Hoare T, Sheardown H. Nanogels of methylcellulose hydrophobized with N-tert-butylacrylamide for ocular drug delivery Drug Deliv. Transl. Res. (2016) 6:648–659. DOI 10.1007/s13346-016-0337-4. © Controlled Release Society 2016

Note: Some symbols and text may have become corrupted during export (e. g. μ exports to m). Please contact the corresponding author for clarification.

Nanogels of methylcellulose hydrophobized with N-tert-butylacrylamide for ocular drug delivery

Marion Jamard¹ & Todd Hoare² & Heather Sheardown²

Corresponding author: Heather Sheardown sheadow@mcmaster.ca

¹School of Biomedical Engineering, McMaster University, 1280 Main Street West, Hamilton, Ontario L8S 4L8, Canada

² Department of Chemical Engineering, McMaster University, 1280 Main Street West, Hamilton L8S 4L8, Canada

Abstract While eye drops account for the majority of ophthalmic formulation for drug delivery, their efficiency is limited by rapid pre-corneal loss. In this study, we investigate nanogel suspensions in order to improve the topical ocular therapy by reducing dosage and frequency of administration. We synthesized self-assembling nanogels of 140 nm by grafting side chains of poly(N-tert-butylacrylamide) (PNtBAm) on methylcellulose via cerium ammonium nitrate. Successful grafting of PNtBAm onto methylcellulose (MC) was confirmed by both NMR and ATR. Synthesized molecules (MC-g-PNtBAm) self-assembled in water driven by hydrophobic interaction of the grafted side chains creating colloid solutions. Materials were synthesized by changing feed ratios of acid, initiator and monomer in order to control the degree of hydrophobic modification. The nanogels were tested for different degrees of grafting. Viability studies performed with HCE cells testified to the biocompatibility of poly(N-tert-butylacrylamide) grafted methylcellulose nanogels. Dexamethasone was entrapped with an efficiency superior to 95 % and its release presented minimal burst phase. Diffusion of drug from the nanogels was found to be delayed by increasing the degree of grafting. The release profile of the entrapped compound from the MC-g-PNtBAm nanogels can thus be tuned by simply adjusting the degree of hydrophobic modification. MC-g-PNtBAm nanogels present promising properties for ocular drug delivery.

Keywords Methylcellulose · Polysaccharide · Hydrophobization · Nanogels · Ophthalmic · Drug delivery/ release

Introduction

Topical administration is the most common delivery method employed to treat diseases of the anterior segment of the eye. Due to their convenience, eye drops account for approximately 90 % of commercially available ophthalmic formulations [1, 2]. However, the eye is characterized by its high resistance to foreign substances [3]. Rapid drainage through the nasolacrimal duct, constant dilution by the turnover of tears, and low drug permeability across the corneal epithelium [4, 5] significantly limit the efficiency of common topical formulations. Only 1 to 5 % of the drug reaches the intraocular tissues [6, 7]; the remainder of the drug dosage undergoes spillage or nonproductive systemic uptake the latter of which may result in serious adverse effects [8, 9]. Multiple daily administrations are then often necessary to achieve therapeutic efficacy, resulting in a higher potential for side effects and lower patient compliance. Thus, there is a need to improve ocular bioavailability and extend drug effect in targeted tissues. The drug delivery system should allow for prolonged contact time with the precorneal tissue to enhance corneal penetration, while remaining patient friendly.

There is a growing interest in the development of particulate topical formulations [3, 6, 10–15] to overcome the limitations associated with topical administration methods. Indeed, nanoparticle carriers have been shown to improve drug stability in water and prolong drug activity through the controlled release of encapsulated compounds [3, 4, 10, 15, 16]. Hydrophilic nanogels are easily dispersed in aqueous media forming freeflowing opalescent solutions [17–21] and can thus be administered in liquid dosage forms for parenteral or mucosal administration. Able to encapsulate bioactive compounds and release their payload in a controlled fashion [20, 22], such formulations could improve topical ocular therapy by reducing dosage and frequency of administration. Furthermore, previous studies demonstrated that the drug penetration capability across the cornea could be significantly improved when the particle size of nanoparticles is decreased [23–25].

However, a few limitations remain in the currently developed nanoparticle formulations. The synthesis of those nanogels often involves harsh conditions, including the use of organic solvents and high temperatures which can be detrimental to the encapsulated compound [26]. Furthermore, an additional step is needed in most cases to induce nanogel formation. When entrapped in particulate systems, the payload is sometimes released within a day with a significant burst phase [14, 15, 27, 28].

As natural biomaterials, polysaccharides are highly stable, non-toxic, hydrophilic, and biodegradable. Numerous studies have been conducted on polysaccharides and their derivatives for potential application as nanoparticle drug delivery systems [28–30]. The modification of polysaccharides with hydrophobic moieties has been shown to result in the formation of nanogels in an aqueous environment through a selfassembly process driven by hydrophobic interaction. The resulting stable monodispersed hydrogel nanoparticles have been used to encapsulate and release various bioactive compounds

[31–34]. By formation of hydrophobic domains within the nanoparticles in aqueous solution, the hydrophobic moieties are expected to efficiently encapsulate hydrophobic compounds, thus enhancing their water solubility [23–25, 35, 36].

The aim of the present work was to hydrophobically modify methylcellulose (MC) in order to form nanogels for use as a drug carrier for improving ophthalmic drug availability. MC is a water-soluble cellulose derivative with a heterogeneous structure consisting of regions substituted with methoxy groups called hydrophobic zones and less substituted regions called hydrophilic zones [37]. This natural biopolymer has been extensively investigated for biomedical applications, including ocular applications due to its biocompatibility and degradability [38–40] and was thus chosen as the base polysaccharide for the nanogels. N-substituted acrylamides are temperature-sensitive monomers, which can produce thermosensitive polymeric structure and have been repeatedly used for the synthesis of biomaterials [41–44], especially for hydrophobization [41–47]. N-tert butylacrylamide (NtBAm) was thus selected as the hydrophobic moiety.

Nanogels were synthesized by grafting hydrophobic branches of poly(N-tert-butylacrylamide) (PNtBAm) onto methylcellulose, using cerium ammonium nitrate (Fig. 1). Often used on polysaccharides [48–50], grafting via cerium ammonium nitrate (CAN) results in high grafting efficiency [51–56] with minimal undesirable side reactions [57–59] and has the advantage of being carried out in water at room temperature. Cellulose and its derivatives have previously been grafted using CAN with poly(N-isopropylacrylamide) [60], polyacrylonitrile [61–63], methylmethacrylate [63], and poly(acrylic acid) [64]. The nanogels prepared with PNtBAm grafted MC (MC-g-PNtBAm) were synthesized with varying feed ratios of monomer, initiator, and acid in order to examine the impact of those factors on the amount of NtBAm grafted, and how the degree of hydrophobic modification would influence the nanogel properties. MC-g-PNtBAm nanogels were then characterized including morphological structure, size, biocompatibility with HCE cells, and loaded with dexamethasone to evaluate their potential for delivery of drugs.

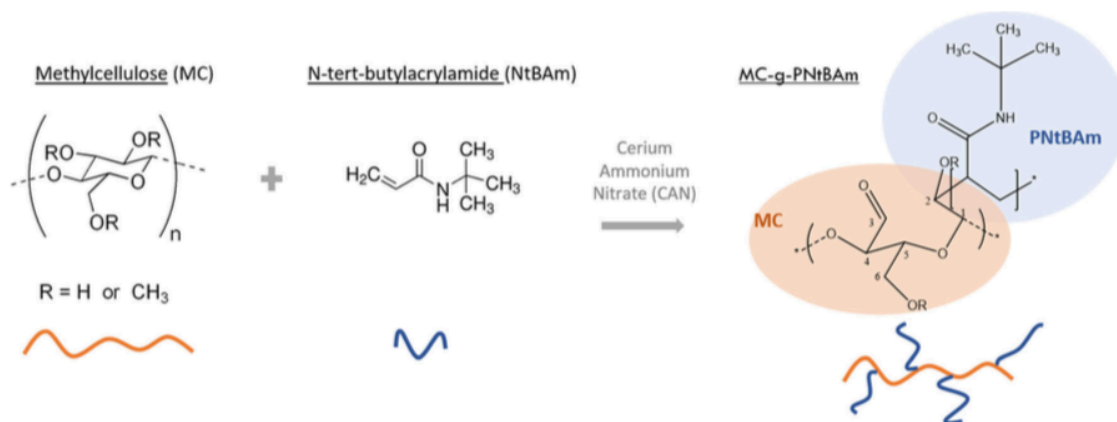


Fig. 1 Synthesis of MC-g-PNtBAm copolymers. Grafting reaction of NtBAm on MC via cerium ammonium nitrate

Experimental section

Materials

Methylcellulose (MC) Metholose SM-15 was purchased from Shin-Etsu (Totowa, NJ, USA). N-tert-butylacrylamide (NtBAm), Cerium ammonium nitrate (CAN) and dimethyl sulfoxide-d6 (DMSO-d6) were purchased from SigmaAldrich, and Dexamethasone from Sigma Life Science (D1756) (St Louis, MO, USA). Phosphate-buffered saline (PBS) ten-time concentrate was obtained from BioShop (McMaster University – Ontario, Canada). Nitric acid 70 % was bought from EMD Chemical Inc. Vybrant MTT cell proliferation assay kit and LIVE/DEAD viability/cytotoxicity kit were purchased from Molecular Probes by Life Technologies (Eugene, Oregon, USA) and cell growth media—Keratinocyte-SFM came from Gibco by Life Technologies (Grand Island, NY, USA). Human corneal epithelium cells [65] (hCECs) were the kind gift of Dr. May Griffith.

Preparation of MC-g-PNtBAm nanogels

In a round bottom flask, 0.25 g of MC was dissolved in 50 mL of water (0.5 % w/v). NtBAm at different ratios was incorporated into the solution, and when dissolved, nitric acid (at 70 %) was added. The mixture was purged with nitrogen for 30 min. Finally, CAN dissolved in 1 mL of purified water prepared in a Millipore Milli-Q system was syringed into the solution to start the polymerization. The reaction was left stirring at room temperature for 24 h, followed by extensive dialysis (Pre-wetted RC tubing 3.5 kDa, Spectrum Laboratories) to remove any unreacted compound. Various amounts of NtBAm, nitric acid, and CAN were used to synthesize the nanogels as shown in Table 1.

Table 1 Concentrations of acid, initiator, and monomer used to synthesize MC-g-PNtBAm

		Nitric acid	CAN	NtBAm
1		75 μ L	50 mg	50 mg
	Concentration	2.52×10^{-2} mol/L	1.82×10^{-3} mol/L	7.86×10^{-3} mol/L
2		150 μ L	150 mg	250 mg
	Concentration	5.04×10^{-2} mol/L	5.48×10^{-3} mol/L	3.94×10^{-2} mol/L
3		300 μ L	250 mg	450 mg
	Concentration	1.01×10^{-1} mol/L	9.12×10^{-3} mol/L	7.08×10^{-2} mol/L

FT-IR analysis

FT-IR spectra of freeze dried samples were measured (Bruker Vertex 70 Bench and HTS plate reader) as KBr discs in the range of 400 to 4000 cm^{-1} .

NMR analysis

Freeze dried materials (Labconco 7,752,020) were dissolved in DMSO-d6 and analyzed by nuclear magnetic resonance (NMR, Bruker AVANCE 600 MHz NMR spectrometer). Nanogel nomenclature was based on the degree of hydrophobization, calculated as the

average number of NtBAm monomer for 100 anhydroglucose units (AGU) of the MC following the equation below. For example, MC-gPNtBAm_50% denotes a nanogel with 50 NtBAm units for 100 AGU.

$$DH = \frac{A_{NtBAm}}{A_{MC}} \times 100$$

A_{NtBAm} indicates the area under the peak at 1.26 ppm corresponding to the tert-butyl group = 9 hydrogens for each NtBAm monomer.

A_{MC} indicates the area under the peak at 2.81 ppm corresponding to the hydrogen in C2 position = 1 hydrogen for each AGU.

Particle size measurements

Mean particle size was measured by single nanoparticle tracking using a Malvern NanoSight LM10 instrument.

Transmission electron microscopy

After diluting the sample 10-fold or 40-fold with purified water, 5 μ L of the suspension was spread on 200 mesh Formvarcoated copper grids without staining and allowed to dry under ambient atmospheric conditions. The morphology of nanogel samples was viewed and photographed using transmission electron microscopy (TEM, JEOL 1200EX TEMSCAN) with 80 kv electron beam.

Loading of dexamethasone

To load dexamethasone into the nanogels, MC-g-PNtBAm synthesis was performed in a 0.01 % w/v aqueous solution of dexamethasone. The nanogel suspension was then ultracentrifuged (Sorvall WX90) at 50,000 rpm at 23 °C for 30 min. The amount of drug in the supernatant was measured by high performance liquid chromatography (HPLC, Waters 2707 Autosampler, 1525 Binary HPLC Pump, 2489 UV/ Visible detector, Waters Atlantis dC18, 5 μ m column) using 1 mL/min isocratic flow rate of 40:60 (v/v) acetonitrile:water, a 10- μ L sample injection volume and a 254-nm detection wavelength. Sample concentrations were determined based on a standard calibration curve of dexamethasone in 40:60 (v/v) acetonitrile/water.

The loading efficiency of dexamethasone into the nanogel particles was calculated using the following equation:

$$\text{Loading efficiency (\%)} = 100 \times \frac{\text{Initial amount of drug} - \text{Amount of drug in supernatant}}{\text{Initial amount of drug}}$$

In vitro release of dexamethasone

The in vitro release of dexamethasone from the nanogels was evaluated in phosphate-buffered saline. A dialysis membrane (molecular weight cutoff 3500 Da, Spectra/ Por, Spectrum laboratories) was first soaked in the dissolution medium and tied at one end. The dispersion of drug-loaded particles in PBS was placed into this bag and its other end was tied. The bag was immersed into 5 mL of PBS maintained at 32 ± 1 °C by a shaking water bath. Released dexamethasone was sampled at selected time intervals by removing the release medium and replacing it with fresh pre-warmed PBS. Concentrations of dexamethasone in the releasate were determined by HPLC using the method described above. The release profile of dexamethasone was compared with a control sample in which dexamethasone was dissolved directly in PBS and placed on the dialysis membrane. All measurements were performed in triplicate and plotted as mean \pm SD.

Cell toxicity studies

The determination of cell viability is a common assay to evaluate the in vitro cytotoxicity of biomaterials. In the present study, cell viability was assessed by the MTT assay and Calcein AM–Ethidium homodimer-1 staining assay.

MC-g-PNtBAm samples were sterilized by incubation in 1 % of penicillin-streptomycin and exposure to UV irradiation (254 nm) overnight. Human corneal epithelial cells (HCECs), the kind gift of Dr. May Griffith, were seeded onto 96-well plates at a density of 5000 cells/well and cultured in 100 μ L of keratinocyte serum free medium for 24 h in a CO incubator. The spent medium was replaced with nanogel formulations and diluted with culture

medium to give a methylcellulose concentration of 0.225 and 1.125 mg/ml. After 48 h of incubation at 37 °C, the nanogel containing media was replaced with 100 μ L of PBS and 10 μ L of MTT stock (5 mg/ml) or 100 μ L of calcein AM-ethidium homodimer-1 working solution (2 μ M calcein AM, 4 μ M ethidium homodimer-1).

For the calcein AM–Ethidium homodimer-1 assay, the cells were incubated for 45 min at room temperature. For the MTT assay, the cells were incubated for 4 h. Then, the supernatant was replaced by 50 μ L of DMSO and incubated at 37 °C for 10 min. The resultant solutions were measured in a microplate reader (Tecan Infinite 200 Pro) at 540 nm (MTT assay) or 530 and 645 nm (Calcein and Ethidium) in a microplate reader (Tecan Infinite 200 Pro).

Cell viability was expressed as percentage of absorbance relative to control comprising

cells not exposed to the nanogels. Experiments were performed on four different nanogels at two concentrations with six replicate wells for each sample and control per assay.

Result and discussion

Synthesis of MC-g-PNtBA_m nanogels

Grafting of PNtBA_m side chains from a MC backbone in an aqueous solution produced nanogels through a selfassembly mechanism driven by hydrophobic interactions. At the first stage of the synthesis process, radicals are formed along the MC backbone from which chain polymerization of NtBA_m occurs. When the hydrophobic modification reaches a critical degree, the PNtBA_m chains gather to form hydrophobic domains, thus driving selfassembly of the MC-g-PNtBA_m molecules into nanogels. Based on Akiyoshi et al., it was proposed that the selfassembled particle was as a nanosized hydrogel, in which the polysaccharide chains are cross-linked noncovalently by associating hydrophobic moieties forming a polycore model [66]. As no macroscopic precipitation takes place in this process, it is suggested that the PNtBA_m chains are mostly contained in the bulk of the nanogels while the periphery of the nanoparticles is mostly methylcellulose, which stabilizes the colloid.

Successful grafting of PNtBA_m onto methylcellulose was confirmed by both NMR and FTIR. The NMR spectra showed the peak for the butyl groups at 1.26 ppm (Fig. 2). FTIR analysis revealed the appearance of a peak at 1651 cm⁻¹ assigned to the characteristic absorption of the carbonyl groups of the ring opening of the MC backbone. An absorbance band at 1510 cm⁻¹ is attributed to the secondary amine bending and peaks at 1390/1361/ 1224 cm⁻¹ are associated with the butyl groups of PNtBA_m (Fig. 3).

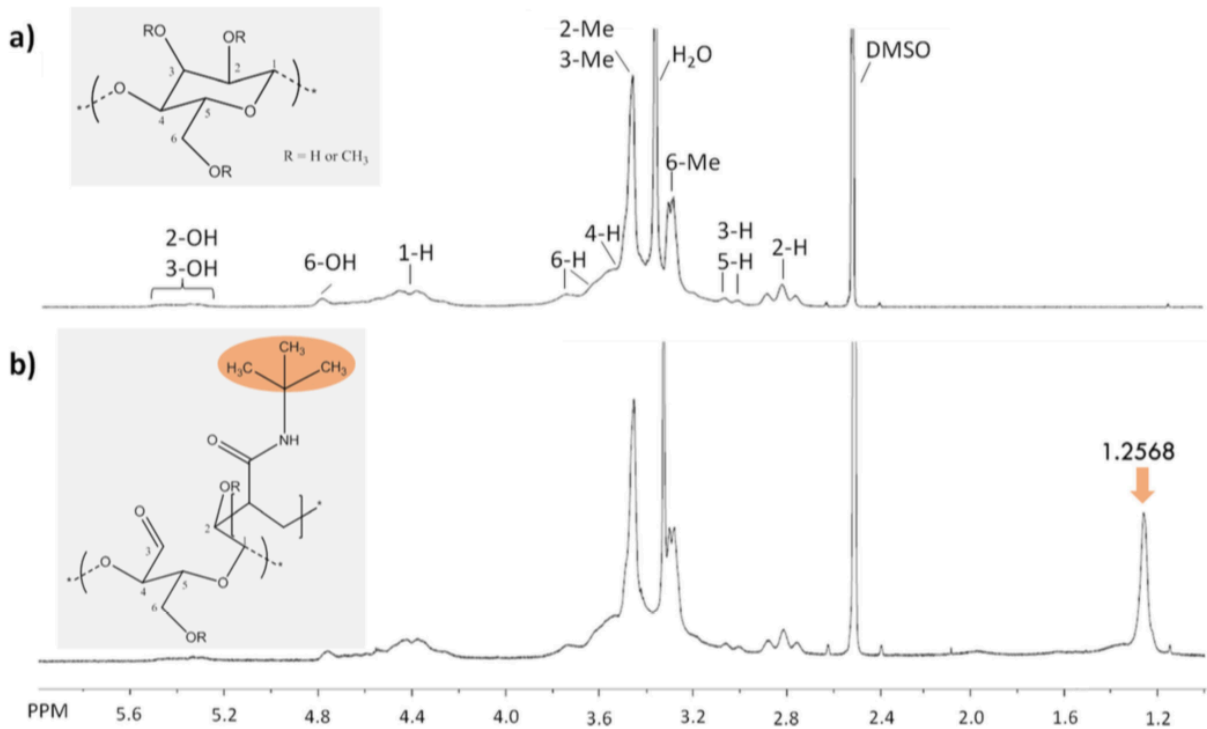


Fig. 2 NMR spectra of a MC and b MC-g-PNtBAm

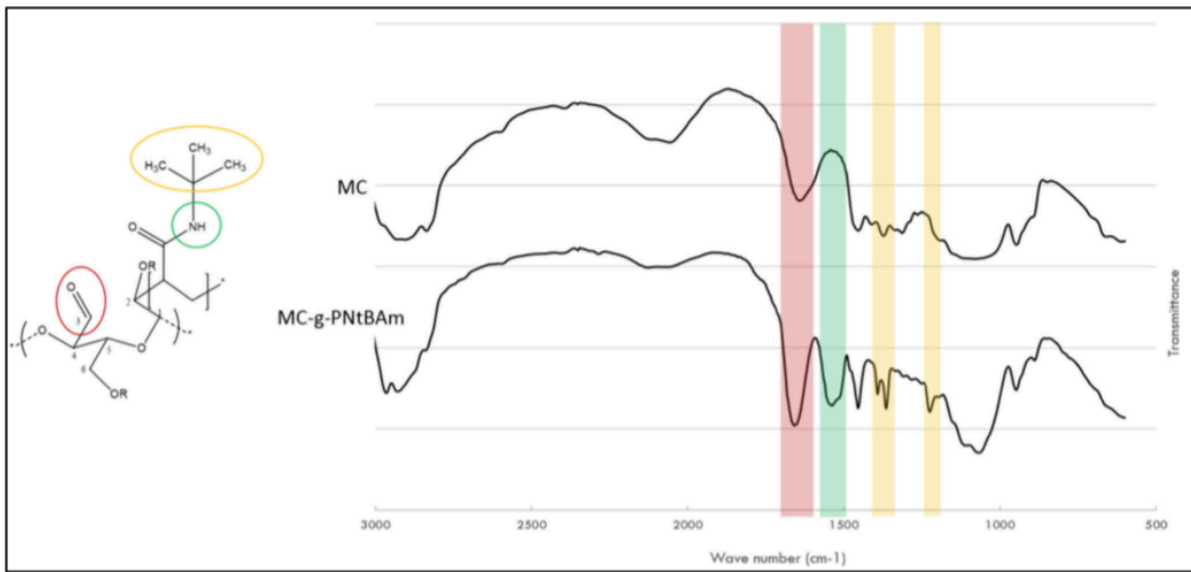


Fig. 3 FTIR spectra of MC and MC-g-PNtBAm

Effect of monomer, initiator, and acid concentrations on the degree of hydrophobization

Different materials were synthesized by changing acid, initiator, and monomer concentrations, with the aim of looking into the impact of those factors on the degree of hydrophobic modification and the corresponding properties of the nanogels.

The amount of hydrophobic modification varying acid and initiator concentrations was compared with a constant concentration of NtBAM at its maximum solubility in solution (9 g/L). With increased acid concentration, hydrophobic grafting increased. However, the impact is limited at low initiator concentration as shown in Fig. 4a. Similarly, increasing the initiator concentration increases the grafting percentage, but does not have an impact at low acid concentration (Fig. 4b). Supplementary data support these trends at different values of monomer, initiator, and acid concentrations (Figs. A1, A2, and A3).

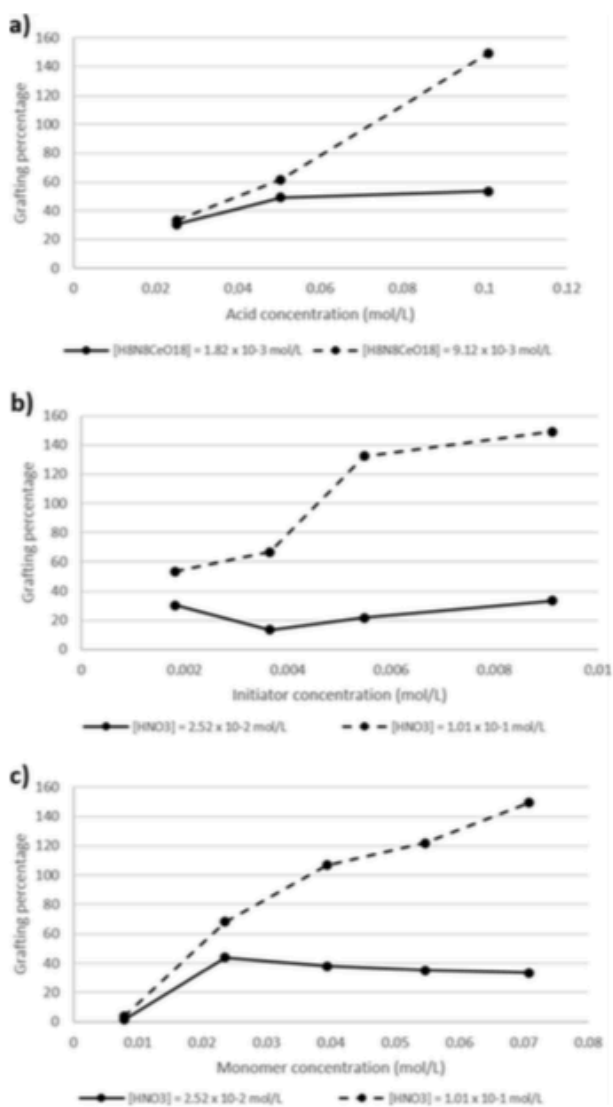


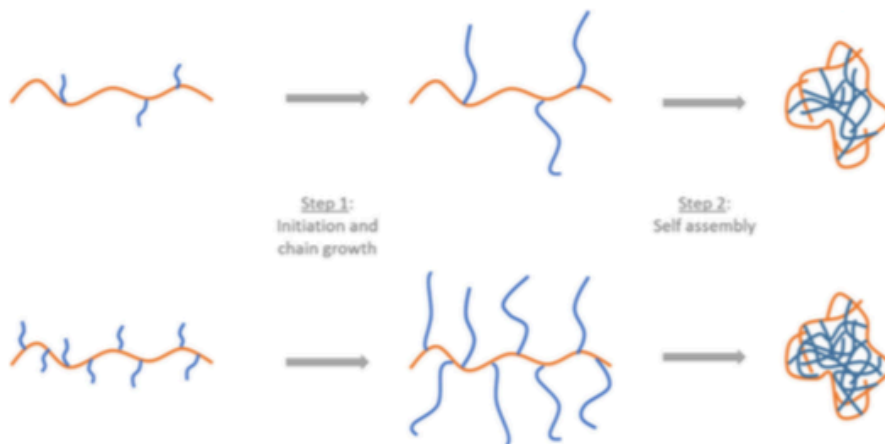
Fig. 4 Degree of hydrophobization when increase in a nitric acid concentration, b cerium ammonium nitrate concentration, and c NtBAM concentration

The role of nitric acid in the grafting mechanism is to prevent hydration of the ceric(IV) ions [60]. Thus, in the presence of insufficient concentrations of nitric acid, ceric(IV) ions are hydrated and are hence inactive for generating active sites on the MC for grafting of

PNtBAm. Thus, increasing the feed concentration of initiator to 9.12×10^{-3} mol/L does not increase initiation unless there is additional acid available to minimize hydration. An excess of nitric acid compared to initiator did not have an impact on the grafting reaction (Fig. 4a). The trends observed when increasing NtBAm concentration in solution with high initiator concentration (Fig. 4c) suggest that the concentration of initiator requires a matching concentration of nitric acid to allow for all of the CAN to be active. Indeed, in the presence of high acid concentration, grafting increased consistently by increasing the amount of monomer, while it plateaued with a lower acid concentration. In accordance with previous studies [60, 61], it was also shown that with sufficient active ceric(IV) ions to initiate, increasing monomer concentration increased the grafting degree. These observations clearly indicate that sufficient nitric acid has to be available in the mixture to maintain the oxidation potential of ceric(IV); otherwise, the efficiency of ceric(IV) ions is changed significantly.

Based on the trends, it appears that initiation is the key to grafting efficiency. Indeed, at high acid and monomer concentrations, increasing the amount of CAN increases the amount of NtBAm grafted on MC (Fig. 4b). Higher initiation implies that more growing chains are visible on which the monomers can graft before the hydrophobic modification reaches a sufficiently high degree to trigger self-assembly of the MC-g-PtBAm molecules into nanoparticles. Then, graft polymerization stops as the grafted chains are gathered into the hydrophobic domains where they are no longer accessible to the remaining monomers in the aqueous phase (Fig. 5).

Fig. 5 Effect of initiation on the degree of hydrophobization



Size and morphology of the MC-g-PNtBAm nanogels

The effect of the degree of hydrophobization (DH) on the nanogel morphology was studied using Nanosight and TEM. Irrespective of the DH, Nanosight revealed that all materials were unimodal and monodispersed self-aggregates, as reported for other self-assembled particles made of hydrophobized polysaccharides [66]. In the swollen state, the nanogels are 143 ± 22 nm, with no significant impact of the DH on their average size.

Longer grafted chains have been reported to lead to larger particles [67] and higher hydrophobicity can reduce swelling in water leading to smaller particles [32, 66]. We postulate that the absence of impact of grafting on the nanogel size is likely due to a tradeoff between these two effects. An optimum size range is required to enhance the bioavailability of the drug at ocular surface or disease site. Smaller particles (100 nm) were shown to exhibit the highest uptake compared to larger particles (800 and 1000 nm) and particles of 100 nm were able to penetrate the corneal barrier [68]. The MC-g-PNtBAm nanogels, at 140 nm, thus seem to be in the suitable range for ocular drug delivery.

The nanogels were observed under TEM for different grafting percentages and appeared monodispersed with a spherical morphology (Fig. 6). When suspended in water, their size was smaller than in swollen state and increased from 10 nm to about 100 nm with increasing DH. Indeed, the degree of hydrophobic modification would be expected to impact the water content of the nanoparticles. A high DH implies more hydrophobic domains which decrease the swelling capacity. Therefore, when dried for TEM observation, the nanogel size was reduced accordingly. For example, the selfaggregate of A3I3M3 is composed of 37 % (by volume) polysaccharide and 63 % (by volume) water. Hence, the selfaggregate is regarded as a nanosize hydrogel. Its density increases with the DH, the MC chain behaving as an expanded flexible coil [66, 69].

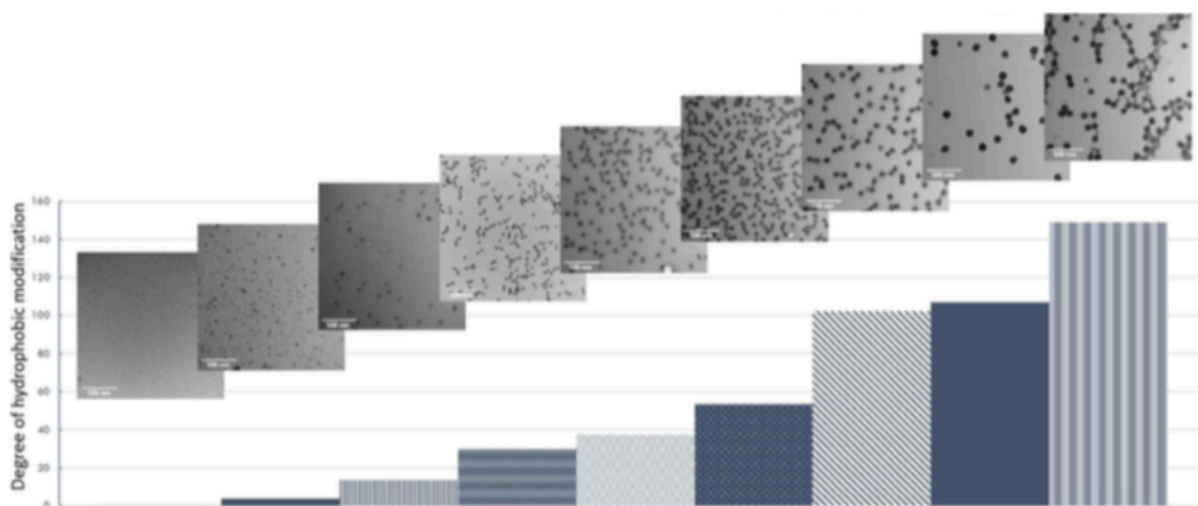


Fig. 6 Morphology of the MC-g-PNtBAm nanogels with different degrees of hydrophobic modification. Scale bar 500 nm

Viability studies

A preliminary biocompatibility test of the nanogels was carried out using human corneal epithelial cells. The nanogels were tested for different degrees of grafting at concentrations of 2.5 mg and 0.5 mg/mL of media for 48 h. After incubating for 48 h, the relative cell viability was higher than 90 % for all of the nanogels, indicating that their presence did not negatively impact cell viability (Fig. 7a). Percentages above 100 % are

due the fact that the data is expressed relative to the control. The MTT assay verified that there was no negative effect on the metabolism (Fig. 7b). The cells continue to proliferate in the presence of the material at a similar rate. Figure 8 shows the morphology of the cells incubated in the presence of MC-g-PNtBAm_149% compared to the control cells.

Fig. 7 Comparison of **a** cell viability in the presence of 1.125 mg/mL MC-g-PNtBAm nanogels and **b** metabolism in the presence of 1.125 and 0.225 mg/mL MC-g-PNtBAm nanogels. Data expressed as a percentage relative to control comprising cells not exposed to the nanogels

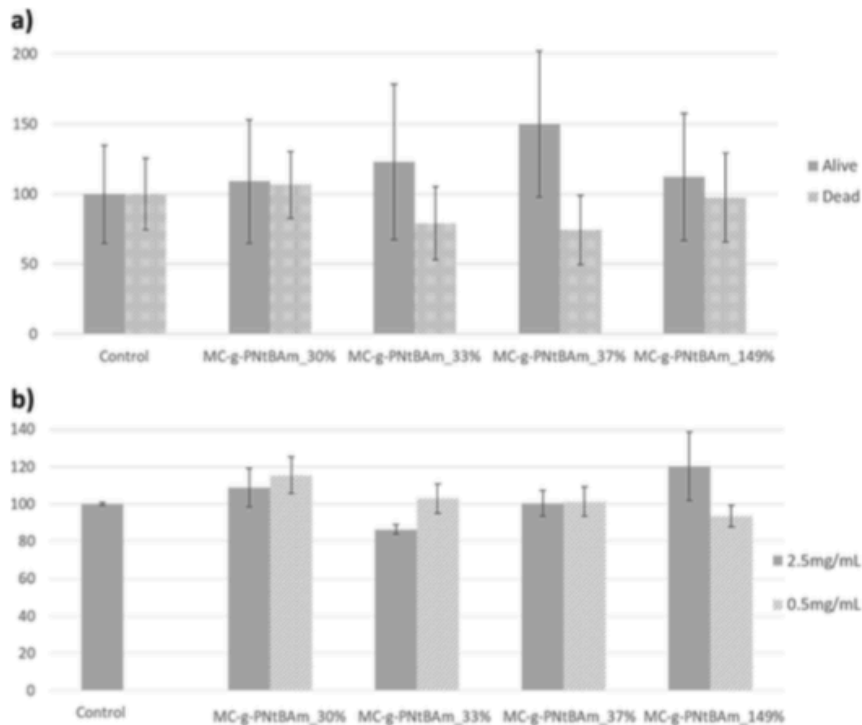
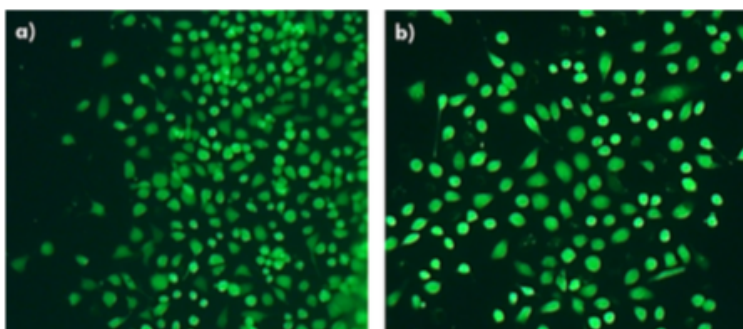


Fig. 8 Cells after 48 h incubation **a** control **b** with MC-g-PNtBAm_149%



Dexamethasone encapsulation

Four materials were chosen to perform a drug encapsulation and release study. The nanogels were loaded with dexamethasone during their synthesis: NtBAm grafting was performed in an aqueous solution of dexamethasone, and the drug was entrapped during the self-assembly of MC-g-PNtBAm. It could be seen from Table 2 that all materials showed an encapsulation efficiency superior to 95 %. As the binding constants have been

reported to become larger with increase in the hydrophobicity of the probes [32], this high complexation of dexamethasone with the nanogel is believed to be mainly driven by hydrophobic interaction [70]. The drug would thus mostly be entrapped within the hydrophobic domains formed by the PNtBAm chain self-aggregates.

Table 2 Loading efficiency of dexamethasone into MC-g-PNtBAm nanogels as a function of feed composition and grafting degree

Feed composition	Entrapment (%)
MC-g-PNtBAm_30%	96.13 ± 0.07
MC-g-PNtBAm_33%	99.84 ± 0.01
MC-g-PNtBAm_54%	98.56 ± 0.06
MC-g-PNtBAm_149%	98.84 ± 0.03

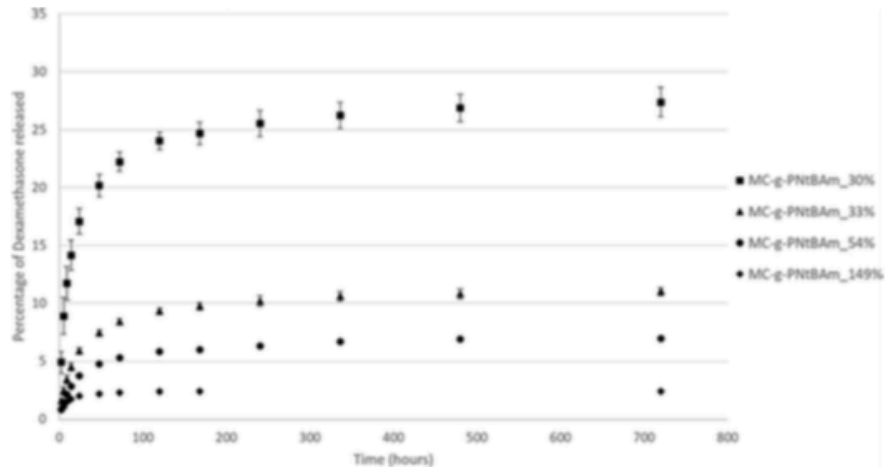
In vitro release of dexamethasone

With simple eye drops, it is not possible to maintain therapeutic concentration on the ocular surface for a prolonged time, and frequent dosing often leads to compliance failures as well as an increased risk of side effects. A sustained drug release system has the potential to improve patient compliance through a reduction in the frequency of administration.

Release from the nanogels was evaluated using the model ophthalmic drug dexamethasone. Dexamethasone, loaded into MC-g-PNtBAm nanogels, was released at 32 ± 1 °C in PBS to mimic the front of the eye conditions. The release profiles of dexamethasone-loaded nanogels with different degrees of grafting were compared with that of a control sample of dexamethasone dissolved directly in PBS, in order to ensure that the release profile was not an artifact of the method.

The cumulative release of dexamethasone from the different samples was plotted as a function of time is shown in Fig. 9. The nanogels showed release profiles that were characterized by a very slight initial burst followed by a sustained-release phase. The first release region presumably corresponds to drugs soaked into the hydrophilic MC part of the nanogels, or drugs encapsulated near the surface [71] whereby a quick release should be expected to occur. As a result, less swollen particles with higher DH show a smaller burst. The nanogels exhibited the burst release during the initial 48 h, releasing from 2.5 to 20 % of the drug.

Fig. 9 Release profiles of dexamethasone from MC-g-PNtBAM nanogels with different degrees of hydrophobic grafting



The second stage is remarkably slower, remaining relatively steady until the release assay is fully carried out. This sustained-release phase most likely corresponds to the diffusional release of the drugs from the hydrophobic PNtBAM domains of the nanogels. It was found that different release profiles could be obtained depending on the degree of grafting. The more NtBAM was grafted, the slower the drug was released.

The release rate appeared to reach a plateau during the final phase (after 7–20 days depending on the material), with a cumulative release that did not equal the total amount of dexamethasone loaded into the nanogels. This stage has been observed in previous release studies from aggregates of hydrophobized polysaccharides [72–76] and was attributed to the reduced concentration gradient. Only up to 28 % of the dexamethasone was released in the time frame of the study, but the study was terminated as the nanogels are expected to be cleared from the surface of the eye by 30 days.

A higher degree of grafting presumably leads to more hydrophobic domains within the nanogels. The affinity of the dexamethasone for the PNtBAM domains within the nanogel resulted in a delay of the diffusion and release of dexamethasone in solution. The rate of the release can thus be tuned by the degree of hydrophobic modification depending on the application and dosage needed.

Conclusion

Novel MC-g-PNtBAM nanogels were successfully prepared using cerium ammonium nitrate. The mild reaction conditions (no organic solvent, room temperature) are suitable for encapsulation of biological compounds. The ability of these materials to self-assemble prevents the need for an extra step. Grafting degree could be controlled on tuning the nitric acid, CAN, and NtBAM feed ratios, forming spherical particles of 140 nm diameter in water. Viability studies performed with HCE cells demonstrated *in vitro* biocompatibility. As well the synthesized nanogels showed efficient entrapment of

dexamethasone. The drug presented no significant burst phase and was released slowly over several weeks, with a release rate that was tunable with the degree of grafting. Those properties suggest that the MC-g-PNtBAM nanogels may have possible application as ocular drug carriers.

Compliance with ethical standards

Funding The funding support of the Natural Sciences and Engineering Research Council of Canada is gratefully acknowledged.

Affiliations The authors certify that they have no affiliations with or involvement in any organization or entity with any financial interest (such as honoraria; educational grants; participation in speakers' bureaus; membership, employment, consultancies, stock ownership, or other equity interest; and expert testimony or patent-licensing arrangements), or nonfinancial interest (such as personal or professional relationships, affiliations, knowledge, or beliefs) in the subject matter or materials discussed in this manuscript.

Ethical approval The authors certify that appropriate ethical approval was obtained where warranted.

Informed consent The authors certify that where appropriate informed consent was obtained.

References

1. Jansook P, Stefánsson E, Thorsteinsdóttir M, Sigurdsson BB, Kristjánssdóttir SS, Bas JF, et al. Cyclodextrin solubilization of carbonic anhydrase inhibitor drugs: formulation of dorzolamide eye drop microparticle suspension. *Eur J Pharm Biopharm.* 2010;76(2): 208–14.
2. Loftsson T, Hreinsdóttir D, Stefánsson E. Cyclodextrin microparticles for drug delivery to the posterior segment of the eye: aqueous dexamethasone eye drops. *J Pharm Pharmacol.* 2007;59(5):629–35.
3. Diebold Y, Calonge M. Progress in retinal and eye research applications of nanoparticles in ophthalmology. *Prog Retin Eye Res.* 2010;29(6):596–609.
4. Gaudana R, Jwala J, Boddu SHS, Mitra AK. Recent perspectives in ocular drug delivery. *Pharm Res.* 2009;26(5):1197–216.
5. Bozdag S, Weyenberg W, Adriaens E, Dhondt MMM, Vergote V, Vervaet C, et al. In vitro evaluation of gentamicin and vancomycin containing minitablets as a replacement for fortified eye drops. *Drug Dev Ind Pharm.* 2010;36(11):1259–70.
6. Li X, Zhang Z, Chen H. Development and evaluation of fast forming nano-composite hydrogel for ocular delivery of diclofenac. *Int J Pharm.* 2013;448(1):96–100.
7. Patton TF, Robinson JR. Quantitative precorneal disposition of topically applied pilocarpine nitrate in rabbit eyes. *J Pharm Sci.* 1976;65(9):1295–301.
8. Qi H, Chen W, Huang C, Li L, Chen C, Li W, et al. Development of a poloxamer analogs/carbopol-based in situ gelling and mucoadhesive ophthalmic delivery system for puerarin. *Int J Pharm.* 2007;337(1–2):178–87.
9. Urtti A, Pipkin JD, Rork G, Sento T, Finne U, Repta AJ. Controlled drug delivery devices for experimental

- ocular studies with timolol 2. Ocular and systemic absorption in rabbits. *Int J Pharm.* 1990;61(3):241–9. 10.
10. Nagarwal RC, Kant S, Singh PN, Maiti P, Pandit JK. Polymeric nanoparticulate system: a potential approach for ocular drug delivery. *J Control Release.* 2009;136(1):2–13.
11. Sosnik A, das Neves J, Sarmiento B. Mucoadhesive polymers in the design of nano-drug delivery systems for administration by non-parenteral routes: a review. *Prog Polym Sci.* 2014;39(12): 2030–75.
12. Gan L, Wang J, Jiang M, Bartlett H, Ouyang D, Eperjesi F, et al. Recent advances in topical ophthalmic drug delivery with lipidbased nanocarriers. *Drug Discov Today.* 2013;18(5–6):290–7.
13. Li N, Zhuang C, Wang M, Sun X, Nie S, Pan W. Liposome coated with low molecular weight chitosan and its potential use in ocular drug delivery. *Int J Pharm.* 2009;379(1):131–8.
14. Liu R, Sun L, Fang S, Wang S, Chen J, Xiao X, et al. Thermosensitive in situ nanogel as ophthalmic delivery system of curcumin: development, characterization, in vitro permeation and in vivo pharmacokinetic studies. *Informa Healthcare USA.* 2015. doi:[10.3109 /10837450.2015.1026607](https://doi.org/10.3109/10837450.2015.1026607).
15. Abd El-Rehim HA, Swilem AE, Klingner A, Hegazy E-SA, Hamed AA. Developing the potential ophthalmic applications of pilocarpine entrapped into polyvinylpyrrolidone-poly(acrylic acid) nanogel dispersions prepared by γ radiation. *Biomacromolecules.* 2013;14(3):688–98.
16. Liu S, Jones L, Gu FX. Nanomaterials for ocular drug delivery. *Macromol Biosci.* 2012;12(5):608–20.
17. Moya-Ortega MD, Alvarez-Lorenzo C, Concheiro A, Loftsson T. Cyclodextrin-based nanogels for pharmaceutical and biomedical applications. *Int J Pharm.* 2012;428(1–2):152–63.
18. Oh JK, Drumright R, Siegwart DJ, Matyjaszewski K. The development of microgels/nanogels for drug delivery applications. *Prog Polym Sci.* 2008;33(4):448–77.
19. Samah NA, Williams N, Heard CM. Nanogel particulates located within diffusion cell receptor phases following topical application demonstrates uptake into and migration across skin. *Int J Pharm.* 2010;401(1–2):72–8.
20. Sawada SI, Sasaki Y, Nomura Y, Akiyoshi K. Cyclodextrinresponsive nanogel as an artificial chaperone for horseradish peroxidase. *Colloid Polym Sci.* 2011;289(5–6):685–91.
21. Guo Q, Wu Z, Zhang X, Sun L, Li C. Phenylboronate-diol crosslinked glycopolymeric nanocarriers for insulin delivery at physiological pH. *Soft Matter.* 2014;10(6):911.
22. Kettel MJ, Dierkes F, Schaefer K, Moeller M, Pich A. Aqueous nanogels modified with cyclodextrin. *Polymer.* 2011;52(9):1917–24.
23. Rafie F, Javadzadeh Y, Javadzadeh AR, Ghavidel LA, Jafari B, Moogooee M, et al. In vivo evaluation of novel nanoparticles containing dexamethasone for ocular drug delivery on rabbit eye. *Curr Eye Res.* 2010;35(12):1081–9.
24. Li X, Zhang Z, Li J, Sun S, Weng Y, Chen H. Diclofenac/ biodegradable polymer micelles for ocular applications. *Nanoscale.* 2012;4(15):4667.
25. Gupta H, Aqil M, Khar RK, Ali A, Bhatnagar A, Mittal G. Biodegradable levofloxacin nanoparticles for

- sustained ocular drug delivery. *J Drug Target*. 2011;19(6):409–17.
26. Ganguly K, Chaturvedi K, More UA, Nadagouda MN, Aminabhavi TM. Polysaccharide-based micro/nanohydrogels for delivering macromolecular therapeutics. *J Control Release*. 2014;193:162–73.
27. Moya-Ortega MD, Alves TFG, Alvarez-Lorenzo C, Concheiro A, Stefánsson E, Thorsteinsdóttir M, et al. Dexamethasone eye drops containing γ -cyclodextrin-based nanogels. *Int J Pharm*. 2013;441(1–2):507–15.
28. Nagarwal RC, Singh PN, Kant S, Maiti P, Pandit JK. Chitosan nanoparticles of 5-fluorouracil for ophthalmic delivery: characterization, in-vitro and in-vivo study. *Chem Pharm Bull*. 2011;59(2): 272–8.
29. Sinha VR, Kumria R. Polysaccharides in colon-specific drug delivery. *Int J Pharm*. 2001;224(1–2):19–38.
30. Lemarchand C, Gref R, Couvreur P. Polysaccharide-decorated nanoparticles. *Eur J Pharm Biopharm*. 2004;58(2):327–41.
31. Akiyoshi K, Kobayashi S, Shichibe S, Mix D, Baudys M, Wan Kim S, et al. Self-assembled hydrogel nanoparticle of cholesterolbearing pullulan as a carrier of protein drugs: complexation and stabilization of insulin. *J Control Release*. 1998;54(3):313–20.
32. Akiyoshi K, Sunamoto J. Supramolecular assembly of hydrophobized polysaccharides. *Supramol Sci*. 1996;3(1–3):157– 63.
33. Sawada S-I, Nomura Y, Aoyama Y, Akiyoshi K. Heat shock protein-like activity of a nanogel artificial chaperone for citrate synthase. *J Bioact Compat Polym*. 2006;21(6):487–501.
34. Gu X, Schmitt M, Hiasa A, Nagata Y, Ikeda H, Sasaki Y, et al. A novel hydrophobized polysaccharide/oncoprotein complex vaccine induces in vitro and in vivo cellular and humoral immune responses against HER2-expressing murine sarcomas. *Cancer Res*. 1998;58: 3385–90.
35. Yoncheva K, Vandervoort J, Ludwig A. Development of mucoadhesive poly(lactide-co-glycolide) nanoparticles for ocular application. *Pharm Dev Technol*. 2011;16(1):29–35.
36. Stella B, Arpicco S, Rocco F, Burgalassi S, Nicosia N, Tampucci S, et al. Nonpolymeric nanoassemblies for ocular administration of acyclovir: pharmacokinetic evaluation in rabbits. *Eur J Pharm Biopharm*. 2012;80(1):39–45.
37. Arisz PW, Kauw HJJ, Boon JJ. Substituent distribution along the cellulose backbone in O-methylcelluloses using GC and FAB-MS for monomer and oligomer analysis. *Carbohydr Res*. 1995;271(1): 1–14.
38. Bhowmik M, Bain MK, Ghosh LK, Chattopadhyay D. Effect of salts on gelation and drug release profiles of methylcellulose-based ophthalmic thermo-reversible in situ gels. *Pharm Dev Technol*. 2011;16(4):385–91.
39. Li N, Yu M, Deng L, Yang J, Dong A. Thermosensitive hydrogel of hydrophobically-modified methylcellulose for intravaginal drug delivery. *J Mater Sci Mater Med*. 2012;23(8):1913–9.
40. Gupta D, Tator CH, Shoichet MS. Fast-gelling injectable blend of hyaluronan and methylcellulose for intrathecal, localized delivery to the injured spinal cord. *Biomaterials*. 2006;27(11): 2370–9.
41. Ngadaonye JI, Cloonan MO, Geever LM, Higginbotham CL. Synthesis and characterisation of thermo-sensitive terpolymer hydrogels for drug delivery applications. *J Polym Res*. 2011;18(6):2307–24.

42. Liu HY, Zhu XX. Lower critical solution temperatures of Nsubstituted acrylamide copolymers in aqueous solutions. *Polymer*. 1999;40(25):6985–90.
43. Moran MT, Carroll WM, Selezneva I, Gorelov A, Rochev Y. Cell growth and detachment from protein-coated PNIPAAm-based copolymers. *J Biomed Mater Res*. 2007.
44. Yildiz B, Işık B, Kış M. Synthesis and characterization of thermoresponsive isopropylacrylamide-acrylamide hydrogels. *Eur Polym J*. 2002;38(7):1343–7.
45. Musial W, Voncina B, Pluta J, Kokol V. The study of release of chlorhexidine from preparations with modified thermosensitive poly-N-isopropylacrylamide microspheres. *ScientificWorld Journal*. 2012. doi:10.1100/2012/243707.
46. Muramatsu K, Wada T, Hirai H, Miyawaki FS. Poly(Nisopropylacrylamide-co-N-tert-butylacrylamide)grafted hyaluronan as an injectable and self-assembling scaffold for cartilage tissue engineering. *J Biomed Sci Eng*. 2012;5:639–46.
47. Hoffman AS, Stayton PS, Bulmus V, Chen G, Chen J, Cheung C, et al. Really smart bioconjugates of smart polymers and receptor proteins. *J Biomed Mater Res*. 2000;52(4):577–86.
48. Pourjavadi A, Mahdavinia GR, Omidian H. Modified chitosan. I. Optimized cerium ammonium nitrate-induced synthesis of chitosan-graft-polyacrylonitrile. *J of Appl Poly Sci*. 2003;88:2048–54.
49. Zhu Z, Zhuo R. Controlled release of carboxylic-containing herbicides by starch-g-poly (butyl acrylate). *J of Appl Poly Sci*. 2001;81: 1535–43.
50. Fanta GF, Burr RC, Doane WM. Polymerization of alkyl acrylates and alkyl methacrylates with starch. *J of Appl Poly Sci*. 1980;25: 2285–94.
51. McDowall DJ, Gupta BS, Stannett VT. Grafting cellulose of vinyl monomers to cellulose by ceric initiation. *Prog Polym Sci*. 1984;10: 1–50.
52. Pulat M, Isakoca C. Chemically induced graft copolymerization of vinyl monomers onto cotton fibers. *J Appl Polym Sci*. 2006;100(3): 2343–7.
53. Zahran MK. Grafting of Methacrylic acid and other vinyl monomers onto cotton fabric using Ce (IV) ion-cellulose thiocarbonate redox system. *J Polym Res*. 2005;13(1):65–71.
54. Kaizerman S, Mino G, Meinhold LF. The polymerization of vinyl monomers in cellulosic fibers. *Text Res J*. 1962;32(2):136–40.
55. Hebeish A, Kaktouch A, El-Rafie MH. Graft copolymerization of vinyl monomers with modified cotton. II. Grafting of acrylonitrile and methyl methacrylate on acetylated cotton. *J of Appl Poly Sci*. 1971;15:11–24.
56. Gu L, Gu G, Saadet O. Graft copolymerization of acrylic acid onto cellulose: effects of pretreatments and crosslinking agent. *J of Appl Poly Sci*. 2000;80:2267–72.
57. Kubota H, Shiobara N. Photografting of N-isopropylacrylamide on cellulose and temperature-responsive character of the resulting grafted celluloses. *React & Funct Poly*. 1998;37:219–24.

58. Chatterjee S, Sarkar S, Bhattacharyya SN. Colloidal ferric oxide: a new photosensitizer for grafting acrylamide onto cellulose acetate films. *Polymer*. 1993;34(9):1979–80.
59. Chiriac AP, Neamtu I, Cazacu G, Simionescu CI. An investigation of the grafting of cellulose powder with acrylamide under a magnetic field. *Die Angewandte Makromolekulare Chemie*. 1997;246(4224):1–9.
60. Gupta KC, Khandekar K. Temperature-responsive cellulose by ceric(IV) ion-initiated graft copolymerization of Nisopropylacrylamide. *Biomacromolecules*. 2003;4(3):758–65.
61. Ahn HR, Tak TM. Optimization grafting conditions and characterization of methyl cellulose grafted polyacrylonitrile copolymer. *Macromol Res*. 2014;22(3):318–23.
62. Hebeish A, Mehta PC. Cerium-initiated grafting of acrylonitrile onto cellulosic materials. *J Appl Poly Sci*. 1968;12:1625–47.
63. Okieimen FE, Ogbeifun DE. Graft copolymerization of modified cellulose, grafting of acrylonitrile, and methyl methacrylate on carboxy methyl cellulose. *J Appl Polym Sci*. 1996;59(6):981–6.
64. Eromosele IC, Eromosele CO, Zanna HK. Graft copolymerization of acrylic acid on methylcellulose by ceric ion/p-xylene redox pair. *J Appl Polym Sci*. 2002;84(3):500–4.
65. Griffith M. Functional human corneal equivalents constructed from cell lines. *Science*. 1999;286(5447):2169–72.
66. Akiyoshi K, Deguchi S, Tajima H, Nishikawa T, Sunamoto J. Microscopic structure and thermoresponsiveness of a hydrogel nanoparticle by self-assembly of a hydrophobized polysaccharide. *Macromolecules*. 1997;9297(96):857–61.
67. Verma MS, Liu S, Chen YY, Meerasa A, Gu FX. Size-tunable nanoparticles composed of dextran-b-poly(D,L-lactide) for drug delivery applications. *Nano Res*. 2012;5(1):49–61.
68. Qaddoumi MG, Ueda H, Yang J, Davda J, Labhasetwar V, Lee VHL. The characteristics and mechanisms of uptake of PLGA nanoparticles in rabbit conjunctival epithelial cell layers. *Pharm Res*. 2004;21(4):641–8.
69. Funami T, Kataoka Y, Hiroe M, Asai I, Takahashi R, Nishinari K. Thermal aggregation of methylcellulose with different molecular weights. *Food Hydrocoll*. 2007;21(1):46–58.
70. Akiyoshi K, Deguchi S, Moriguchi N, Yamaguchi S, Sunamoto J. Self-aggregates of hydrophobized polysaccharides in water. Formation and characteristics of nanoparticles. *Macromolecules*. 1993;26(12):3062–8.
71. Saldías C, Velásquez L, Quezada C, Leiva A. Physicochemical assessment of dextran-g-poly(ϵ -caprolactone) micellar nanoaggregates as drug nanocarriers. *Carbohydr Polym*. 2015;117:458–67.
72. Guo Y, Zhang L, Li H, Han Y, Zhou J, Wang X. Self-assembly and paclitaxel loading

capacity of α -tocopherol succinate-conjugated hydroxyethyl cellulose nanomicelle. *Colloid Polym Sci.* 2016;294:135–43.

73. Calejo MT, Kjøniksen AL, Maleki A, Nyström B, Sande SA. Microparticles based on hydrophobically modified chitosan as drug carriers. *J Appl Polym Sci.* 2014;131(7):1–11.

74. Vafaei SY, Esmaeili M, Amini M, Atyabi F, Ostad SN, Dinarvand R. Self assembled hyaluronic acid nanoparticles as a potential carrier for targeting the inflamed intestinal mucosa. *Carbohydr Polym.* 2016;144:371–81.

75. Yang Y, Guo Y, Sun R, Wang X. Self-assembly and β -carotene loading capacity of hydroxyethyl cellulose-graft-linoleic acid nanomicelles. *Carbohydr Polym.* 2016;145:56–63.

76. Wang M, Huang M, Wang J, Ye M, Deng Y, Li H, et al. Facile onepot synthesis of self-assembled folate-biotin-pullulan nanoparticles for targeted intracellular anticancer drug delivery. *J Nanomater.* 2016. doi:10.1155/2016/5752921.